

CHANSON, H., AOKI, S., and MARUYAMA, M. (2002). "Unsteady Air Bubble Entrainment and Detrainment at a Plunging Breaker: Dominant Time Scales and Similarity of Water Level Variations." *Coastal Engineering*, Vol. 46, No. 2, pp. 139-157 (ISSN 0378-3839).

Unsteady Air Bubble Entrainment and Detrainment at a Plunging Breaker:
Dominant Time Scales and Similarity of Water Level Variations

Hubert CHANSON

Dept. of Civil Engineering, The University of Queensland, Brisbane QLD 4072, Australia (¹)

Fax : (61 7) 33 65 45 99 - Email : h.chanson@mailbox.uq.edu.au

Shin-ichi AOKI,

and

Mamoru MARUYAMA

Dept. of Architecture and Civil Engineering, Toyohashi University of Technology, Toyohashi, 441- 8580, Japan

Abstract :

At plunging breakers, air bubbles are entrained at the impingement of the water jet, formed at the top of the wave, with the water free-surface in front. During the present study, air bubble entrainment at a pseudo-plunging breaker was investigated at near full-scale and further experimental work studied the bubble detrainment process. Experimental observations included the generation and propagation of waves downstream of the plunge point. Experimental results highlighted a number of unsteady air-water flow patterns and emphasise high levels of aeration : i.e., depth-averaged void fraction of more than 10% next to jet impact in shallow waters. Unsteady bubble injection experiments showed a strong vortical motion induced by the rising bubbles. Altogether the results suggest that a dominant time scale is the bubble rise time d/u_r which cannot be scaled properly with an undistorted Froude model. The study contributes to a better understanding of unsteady bubble entrainment at a pseudo-plunging breaker and the associated vortical circulation.

¹Author to whom the correspondence should be addressed.

CHANSON, H., AOKI, S., and MARUYAMA, M. (2002). "Unsteady Air Bubble Entrainment and Detrainment at a Plunging Breaker: Dominant Time Scales and Similarity of Water Level Variations." *Coastal Engineering*, Vol. 46, No. 2, pp. 139-157 (ISSN 0378-3839).

1. Introduction

Air bubble entrainment by breaking waves is a significant factor in the surf zone under high wave conditions, in terms of water quality and energy dissipation. Air-water mass transfer across the air bubble interface is significant as the net surface area of thousands of tiny bubbles is much greater than the surface area above the bubble clouds (e.g. DANIIL and GULLIVER 1991, WALLACE and WIRICK 1992, CHANSON and CUMMINGS 1994). Recently, AOKI et al. (2000) proposed that air entrainment at plunging breakers may be one of the mechanisms of energy transfer from short waves to long-period waves near the shoreline. Long waves with periods of several minutes have been recognised as an important exciting component to beach erosion, sedimentation in harbours, harbour oscillations (seiching) and oscillations of moored ships in havens (e.g. SAWARAGI 1995, KOMAR 1998).

With plunging breakers, the entrainment of air bubbles is caused by the top of the wave forming a water jet projecting ahead of the wave face and entraining air when it impacts the water free-surface in front of the wave (e.g. LIN and HWUNG 1992, CHANSON and LEE 1997) (Fig. 1). In deep waters, plunging breaking waves may be caused by surface wind shear and constructive wave interference during high winds (e.g. COLES 1967, GRIFFIN 1984, LONGUET-HIGGINS 1988). Such breakers have the ability to entrain a large number of bubbles at great depths (e.g. KANWISHER 1963, KOLOVAYEV 1976, THORPE 1982). In shallow waters, the air entrainment process and bubble residence time are affected by the sloping bottom, but bubble entrainment is still significant as highlighted by the "white water" pattern (Fig. 1B) (also DEANE 1997). The entrained bubbles induce a rise in water level associated with an energy transfer into potential energy while breaker-generated waves propagate in off- and on-shore directions (e.g. FUHRBOTER 1970, HWUNG et al. 1992).

The influence of entrained air on the wave field near the surf zone has not yet been well investigated except for some research on energy dissipation by wave breaking. Since the air bubble entrainment process is not properly scaled by Froude's law, most laboratory experiments tend to underestimate its effects, in particular on the wave field (WOOD 1991, CHANSON 1997). In the present study, air bubble entrainment at a pseudo-plunging breaker was investigated at near full-scale. The pseudo-plunging breaker generated jet impact velocities ranging from 5.6 to 6.4 m/s. For comparison, the breaking wave height in Figure 1B was about 2-3 m corresponding to

CHANSON, H., AOKI, S., and MARUYAMA, M. (2002). "Unsteady Air Bubble Entrainment and Detrainment at a Plunging Breaker: Dominant Time Scales and Similarity of Water Level Variations." *Coastal Engineering*, Vol. 46, No. 2, pp. 139-157 (ISSN 0378-3839).

an impact velocity of about 6 to 7 m/s. The work is focused on the unsteady flow patterns associated with air entrainment and detrainment, as well as the dominant time scales. The results provide new information on the unsteady plunging jet process, the rise in free-surface level caused by air entrainment, the effect on the wave field and the similarity of water level variations.

2. Physical modelling of a plunging breaker

In a physical model, the flow conditions are said to be similar to those in the prototype if the model displays similarity of form, similarity of motion and similarity of forces. For wave motion studies, the gravity effect is usually predominant, and model-prototype similarity is performed with a Froude similitude. If the same fluids are used in both model and prototype, distortions are introduced by effects other than gravity (e.g. viscosity, surface tension) resulting in scale effects.

Considering a single plunging breaker, the characteristic time scale of the initial air entrainment equals d_1/V_1 , where d_1 is the initial water depth and the jet impact velocity V_1 is basically proportional to the square root of the wave height (e.g. CHANSON and LEE 1997). A further time scale is the breaker duration t_{jet} , that is a function of the breaker volume per unit width. The characteristic time scale of air detrainment is the bubble rise time d_1/u_r where u_r is the bubble rise velocity.

Both in the field and in laboratory, entrained bubbles are about millimetric and the rise velocity is nearly constant for bubble diameters ranging from 0.5 to 50 mm (WOOD 1991, CHANSON 1997). As a result, the scale ratio of the characteristic air detrainment time becomes :

$$\left(\frac{d_1}{u_r}\right)_R = L_R \quad (1)$$

where the subscript R denotes the ratio of prototype-to-model quantity and L_R is the geometric scaling ratio. But a Froude model implies that the characteristic times must be scaled by $\sqrt{L_R}$ (e.g. IPPEN 1966, HUGHES 1993, CHANSON 1999). Equation (1) demonstrates that the bubble rise time increases with the water depth and cannot be scaled with a Froude similitude.

CHANSON, H., AOKI, S., and MARUYAMA, M. (2002). "Unsteady Air Bubble Entrainment and Detrainment at a Plunging Breaker: Dominant Time Scales and Similarity of Water Level Variations." *Coastal Engineering*, Vol. 46, No. 2, pp. 139-157 (ISSN 0378-3839).

Numerous experimental studies of air entrainment by plunging jets showed that the volume of entrained air per metre width may be estimated as :

$$q_{\text{air}} \propto (V_1 - V_e)^N \quad (2)$$

where V_e is the onset velocity for air bubble entrainment, and the exponent N is about 3 for low-jet velocities and equals to 2 for high jet velocities (reviews by WOOD 1991, BIN 1993, CHANSON 1997). In freshwater, the onset velocity V_e is about 1 to 3.5 m/s (CUMMINGS and CHANSON 1999). Equation (2) implies that a Froude similitude cannot scale properly the volume of entrained air by using the same fluids in model and prototype (unless $V_e = 0$ and $N = 1$). Small-size models basically underestimate the air entrainment, and sometimes no air entrainment is observed when the plunging jet velocity is smaller than the onset velocity V_e .

A further important time scale is the period of the wave group. Larger wave heights are associated with stronger air entrainment than smaller waves. The rise of water level caused by bubble entrainment will be more significant in the bulge of the group envelop. As a result this effect may generate water level oscillations with a period equal to that of the wave group.

Considering a plunging breaker near the shoreline, the jet flow and the associated boiling flow pattern contribute to set sediment matters into suspension. The strong turbulent mixing, observed in the laboratory and in the field, is further enhanced by the upwelling circulation induced by the rising air bubbles. Subsequently, the combined effects of jet mixing and rising bubbles have a direct impact on the sediment transport processes (e.g. NIELSEN 1984). Physical modelling of the three-phase flow is practically impossible, but at full-scale.

3. Experimental setup

Two series of experiments were conducted with freshwater (Table 1, Fig. 2). The first one was focused on the unsteady plunging jet process, the associated air bubble entrainment and detrainment. A strong boiling flow process was observed (section 4). The second experiment was designed to investigate specifically the boiling phenomenon and the effects of rising bubbles on the flow field (Fig. 2B).

CHANSON, H., AOKI, S., and MARUYAMA, M. (2002). "Unsteady Air Bubble Entrainment and Detrainment at a Plunging Breaker: Dominant Time Scales and Similarity of Water Level Variations." *Coastal Engineering*, Vol. 46, No. 2, pp. 139-157 (ISSN 0378-3839).

In the first series of experiments (Series 1), the plunging jet of the breaker was modelled by an unsteady vertical jet discharging into a 20 m long, 0.8 m wide, 0.6 m deep flume. The pseudo plunging breaker was generated by a known volume of water (0.4 to 1.2 m³) discharging through a rectangular sharp orifice (0.75 m by 0.07 m) located 1.32-m above the flume invert. A sloping beach (1V:6H) was installed at the end of the working section (Fig. 2A). The orifice was closed by a steel gate prior to each experiment. The gate release occurred in less than 0.030 s and the free-falling nappe took less than 0.3 s to reach the water surface. The duration of the pseudo plunging breaker ranged from about 5 to 12 s depending upon the initial water volume (Table 1). For some experiments, air entrainment was reduced by a factor of 2 to 3 by inserting 18- μ m plastic films which were fixed inside the watertank, covered the nappe and inhibited bubble entrainment at the plunge point. (The cellophane sheet surrounded the free-falling nappe like stockings. Tests showed that the cellophane sheet did not affect the falling jet. Its weight was negligible and insignificant compared to the jet momentum.)

In a second series of experiments (Series 2), the process of water level rise due to air entrainment, and the effects of air detrainment, were idealised by an air bubble generator (0.48-m long, $\varnothing = 0.045$ m, air discharge up to 0.62 l/s) installed at the bottom of a 4-m long 0.05-m wide section of the wave flume. The air bubble generator was located next to a rear wall and discharged air bubbles into still water with a known depth ($d_1 = 0.5$ m) (Fig. 2B). (The air flow rate was 0.62 l/s for all experiments.) The other end of the test section was open to the wave flume. The configuration was somehow similar to half of a pneumatic breaker (e.g. STRAUB et al. 1959), but the emphasis was put here on unsteady air injections. (The rear wall acted as a symmetry line, hence only half of a rising cloud was simulated.) Basic experiments included sudden air injection, sudden end to bubble injection, and air injection for a controlled duration, with bubble injection periods ranging from 1 to 20 s. Water level fluctuations were measured at several locations along the flume.

Instrumentation

Flow visualisations, nappe trajectory, impact flow conditions and underwater bubble plume were investigated with two video-cameras : a VHS-C camcorder NationalTM CCD AG-30C (speed: 30 frames/s, shutter: 1/60 &

CHANSON, H., AOKI, S., and MARUYAMA, M. (2002). "Unsteady Air Bubble Entrainment and Detrainment at a Plunging Breaker: Dominant Time Scales and Similarity of Water Level Variations." *Coastal Engineering*, Vol. 46, No. 2, pp. 139-157 (ISSN 0378-3839).

1/1,000 s) and a digital handycam Sony™ DV-CCD DCR-TRV900 (speed: 30 fr/s, shutter: 1/4 to 1/10,000 s, zoom: 1 to 48).

Water depths in the reservoir and in the flumes were measured with pointer gauges, capacitance wave gauges and displacement meter. The wave gauges were Kenek™ capacitance gauges with a 10-Hz response and an accuracy of about 1 mm (tested during on-site calibration). One ultrasonic displacement meter Keyence™ UD300 was also used (range: 0.20 to 1.30 m, response: 10 Hz, accuracy: 1 mm, $\varnothing = 20$ mm). The probes were scanned at 50 Hz for 163.8 s.

The effect of air bubbles on wave gauge and displacement meter readings was tested in a preliminary experiment. Air was introduced at the bottom end of a vertical cylinder installed in a stillwater tank. Tests, performed with void fractions ranging from 0 to 0.10, showed that both wave gauges and displacement meter recorded with a reasonable accuracy the rise in water level induced by the air bubbles. The error was of the same order of magnitude as the bubbly foam thickness formed at the water surface in the cylinder, although the output of the gauge tended to correspond to the level above the foam (Fig. 3). Figure 3 presents measured superelevations above still water as functions of the depth-average void fraction for comparable tests.

In the plunging jet experiment (Series 1), the time origin ($t = 0$) was taken at the instant when the nappe impacted onto the water free-surface. The time t was non-dimensionalised in terms of the bubble rise time that was found to be a dominant time scale : i.e., $T = t/(d_1/u_r)$, u_r being the bubble rise velocity in still water. u_r was the speed of the most frequent bubbles. Distances and depths were non-dimensionalised in terms of the initial water depth : e.g., $X = x/d_1$. The longitudinal origin ($x = 0$) was at the centreline of the vertical nappe (Fig. 2). The instantaneous orifice flow rate was deduced from the water level measurements in the tank. The relationship between water height and water volume was calibrated in-situ with a container of known volume.

A number of verifications were performed to ensure the repeatability and consistency of the experiments. Further details were reported in CHANSON et al. (1999) and MARUYAMA (2000).

CHANSON, H., AOKI, S., and MARUYAMA, M. (2002). "Unsteady Air Bubble Entrainment and Detrainment at a Plunging Breaker: Dominant Time Scales and Similarity of Water Level Variations." *Coastal Engineering*, Vol. 46, No. 2, pp. 139-157 (ISSN 0378-3839).

4. Unsteady flow patterns

4.1 Pseudo plunging breaker

The initial impact was associated with a strong splashing of short duration (i.e. less than 0.4 s) and the generation of a downward underwater bubble plume. The splashing was characterised by very small liquid fractions (i.e. less than 2%), and some droplets would travel up to 2.5-m from the impact point and reach heights in excess of 0.4 m above the initial free-surface level. A similar splashing process was observed during the initial stage of the plunging breaking wave in laboratory (e.g. PERLIN et al. 1996, TULIN and WASEDA 1999).

The initial bubble entrainment was a densely populated bubble plume travelling downwards. The bubble plume took about 0.23 to 0.27 s (i.e. $T = 0.065$ to 0.135) to reach the channel bottom for a 0.4 m water depth with an impact velocity of about 5.8 to 6.1 m/s. As the bubble plume reached the bed, a stagnation point developed and the plume was deflected horizontally (Fig. 2A). A bubbly turbidity current flowed parallel to the bed with clear-water above and the plume front expanded as some bubbles rise (Fig. 4). Figure 4 shows a series of underwater photographs taken during one experiment. The camera was located at $x \approx 2$ m looking at the bubble plume progression. On the last photograph, the rising bubbles almost reached the free-surface. The horizontal bubbly flow ran for a distance of about $x = 1$ to 1.2 m ($X \sim 2.5$ to 5) before most bubbles rise to the free-surface by buoyancy. Slow motion pictures suggested that the celerity of the bubble plume front was about 30 to 45% of the jet impact velocity V_1 , although the plunging jet flow was not fully-developed at stagnation.

This rapid sequence of events was followed by the development of a "boiling" flow pattern next to the plunge point. This flow region was extremely turbulent with a large amount of entrained air bubbles, having the same appearance as a hydraulic jump roller. The "roller" region occupied a large surface area : i.e., $x \leq 1.5$ to 2 m ($X \leq 3$ to 5). The boiling flow pattern lasted typically 3 to 7 s (i.e. $\Delta T = 3$ to 7) longer than the free-falling nappe (i.e. pseudo-plunging breaker). Bubbles were still observed underwater after the disappearance of the boiling flow. Visually most entrained air bubbles disappeared around $t = 35$ to 40 s (i.e. $T = 15$ to 25). A time delay, between the end of pseudo plunging breaker and end of the boiling flow pattern, was observed for all experiments.

CHANSON, H., AOKI, S., and MARUYAMA, M. (2002). "Unsteady Air Bubble Entrainment and Detrainment at a Plunging Breaker: Dominant Time Scales and Similarity of Water Level Variations." *Coastal Engineering*, Vol. 46, No. 2, pp. 139-157 (ISSN 0378-3839).

Shortly after jet impact, a positive surge propagated into the flume. It was followed by a negative surge corresponding to a reduction in the orifice flow rate (e.g. HENDERSON 1966, MONTES 1998). When air entrainment was suppressed, the free-surface levels, measured at several locations along the flume, were in close agreement with theoretical results deduced from the continuity and momentum principles for the bore front and from the equations of Saint-Venant for negative surge (Fig. 5). Figure 5 presents dimensionless water levels y/d_1 as functions of the dimensionless time $T = t/(d_1/u_T)$, where y is the water elevation measured above the (initial) still water level. A value of $u_T = 0.2$ m/s was observed and it is characteristic of the observed millimetric bubbles (e.g. COMOLET 1979, CHANSON 1997). Such a value is used thereafter.

4.2 Unsteady bottom injection of bubbles

In the second series of experiments, air injection generated an immediate water level rise above the injector, that propagated subsequently in the flume (Figs. 6 and 7). Figure 6 shows a photograph of the experiment (Fig. 6A), a sketch of the characteristic stages (Fig. 6B) and time variations of the free-surface profile next to the origin during one experiment (Fig. 6C). Figure 7 presents time variations of water levels at several longitudinal positions with increasing bubble injection times from Figures 7A to 7C. (Note that Figures 7A to 7C have different horizontal scales.)

The results showed a strong effect of the bubble injection time onto the water level fluctuations. For long bubble discharges (i.e. $T_{inj} > 3$), the water level fluctuations were typically categorised into three stages, sketched in Figure 6B and shown in Figure 7. In Stage 1 ($0 \leq T \leq 1$ to 2), the water level rose as a direct result of air injection (Fig. 6A & Fig. 7 for $X = 0.68$). The characteristic time scale seemed to be a function of bubble rising time d_1/u_T . At the origin ($x = 0$), the water level rise reached an equilibrium for $T \sim 1.4$. The water superelevation, measured above still water level, was the addition of flow bulking caused by air injection (i.e. $C*d/(1-C)$) and stagnation pressure resulting from the upward bubbly plume velocity w (i.e. $w^2/(2*g)$). The water level rise propagated in the channel. The propagation speed, measured away from the injector ($x \geq 1$ m, $X \geq 2$), was about 2 to 2.4 m/s that is close to the celerity of a small disturbance $\sqrt{g*d_1}$. The maximum water

CHANSON, H., AOKI, S., and MARUYAMA, M. (2002). "Unsteady Air Bubble Entrainment and Detrainment at a Plunging Breaker: Dominant Time Scales and Similarity of Water Level Variations." *Coastal Engineering*, Vol. 46, No. 2, pp. 139-157 (ISSN 0378-3839).

height measured above still water level seemed to decay hyperbolically with the distance. The dimensionless data were best correlated by

$$Y_{21\max} = \frac{8.30 \cdot 10^{-2}}{(X + 0.954)^{1.687}} \quad 0 < X < 9 \quad (3)$$

where $Y_{21\max}$ is the dimensionless water level rise (above still water), $Y = y/d_1$ and $X = x/d_1$.

In Stage 2 ($2 < T \leq T_{inj}$), a strong vortical circulation with large horizontal velocity component was induced by the vertical upward current generated by the bubble plume. This generated a quasi-steady water level fall near the bubble generator and an associated water level rise at some distance. The horizontal velocity current and water level fall are sketched in Figure 6B middle. The water level fall is also seen in Figures 7B and 7C for $X = 2$ with a trough at $Y = -2.75$. Video-analysis, using air bubbles as tracers, highlighted a region of high velocity next to the trough (water level fall) while the velocities were significantly smaller further downstream.

The Stage 3 took place after switching off the bubble generator (i.e. $T > T_{inj}$). The water level dropped following the propagation of the water level fall initially created near the bubble generator. A negative surge (i.e. a decrease in water level below the still water level) was observed propagating with an average celerity of about 2 m/s. (The negative "wave" is sketched in Figure 6B bottom.) The maximum amplitude of the negative surge occurred at about :

$$T_{22} = T_{inj} + 1.05 * (1.28 - \exp(-0.51 * X)) \quad 0.6 < X < 9 \quad (4)$$

where $T = t/(d_1/u_r)$. Experimental data and Equation (4) are compared in Figure 8. The maximum amplitude of the "negative wave" decayed exponentially with distance and the data may be correlated by :

$$Y_{22\max} = -2.63 \cdot 10^{-3} * \exp(-0.128 * X) - 7.24 \cdot 10^{-4} \quad 0.6 < X < 9 \quad (5)$$

Equations (4) and (5) were validated for finite injection times satisfying $T_{inj} \geq 0.4$. Overall, the water level variations caused by air bubble injection lasted consistently longer than the injection time. The total duration of water level variations was best correlated by :

$$T_{23\max} = 18.4 * (1.11 - \exp(-0.062 * T_{inj})) \quad 0.6 \leq T_{inj} \quad (6)$$

corresponding to a time delay between the air injection end and the end of significant water level fluctuations of about : $T_{23\max} - T_{inj} \sim 2$ to 2.5.

CHANSON, H., AOKI, S., and MARUYAMA, M. (2002). "Unsteady Air Bubble Entrainment and Detrainment at a Plunging Breaker: Dominant Time Scales and Similarity of Water Level Variations." *Coastal Engineering*, Vol. 46, No. 2, pp. 139-157 (ISSN 0378-3839).

For short injection periods ($T_{inj} < 3$), Stage 2 was sometimes eliminated as illustrated on Figure 7A.

Discussion

The results of the Series 2 experiments highlight the strong scale vortical circulation generated by the rising bubbles and air detrainment (Figs. 2 and 6). This process took place also during experiments Series 1, although it could not be observed in such details.

The characteristic time scales of water level changes seemed to be strongly correlated to the bubble rise time d_1/u_r . As the bubble rise velocity is nearly identical in both experiments and actual wave field, the result implies that the water depth must be scaled 1:1. That is, the water depth must be the same in the field and in the laboratory.

5. Discussion

5.1 Effects of air entrainment

With free-falling jets and air bubble entrainment, a significant flow bulking (i.e. water level rise) was observed next to the impact zone. It was generated by an upward displacement of water resulting from air entrainment. For all experiments with free-jets, the water level data were consistently higher than theoretical predictions. The differences imply a depth-averaged void fraction of nearly 12% next to the impact zone and about 4 to 6% at about $X = 1$ to 1.2 downstream of nappe impact for the duration of the breaker with $d_1 = 0.4$ m (Fig. 9). Figure 9 presents time variations of the depth-averaged air content C . Note that one set of data marked ($X = -0.275$) was measured at the rear wall ($x = -0.11$ m, Fig. 2A). Figure 9 shows that the void fraction was constant in average for the duration of the plunging breaker at a given location. Further it was found that the water level rise drops near $x = 1$ m ($X = 2.5$), and a similar observation was made during experiments Series 2.

The results of wave data analysis suggests further that air entrainment affects the wave field, in particular the more energetic waves. Figure 10 presents a typical FFT analysis conducted on the differential wave signals of two experiments for identical initial conditions with and without air entrainment : i.e., {experiment with air

CHANSON, H., AOKI, S., and MARUYAMA, M. (2002). "Unsteady Air Bubble Entrainment and Detrainment at a Plunging Breaker: Dominant Time Scales and Similarity of Water Level Variations." *Coastal Engineering*, Vol. 46, No. 2, pp. 139-157 (ISSN 0378-3839).

entrainment} - {experiment with plastic sheets}. (The time origins were set on the first wave crest.) Figure 10A shows the energy spectra and Figure 10B shows the ratio for energy for frequencies between 0.49 and 0.78 Hz to the total wave energy for the experiment with air entrainment. Figure 10A highlights three dominant frequency ranges : around 0.18 Hz which corresponds to the duration of the pseudo-breaker (about 7-8 s), around 0.5 to 0.7 Hz, and around 2 Hz. In Figure 10A, the second peak (0.5-0.7 Hz) is observed at each gauge and the writers hypothesise that the corresponding wave period (i.e. about 1.6 s) is close to the average bubble rise time d_1/u_r . That is, Figure 10A suggests an increase in wave energy in presence of air entrainment at the pseudo-breaker. Further, the energy ratio for the frequencies between 0.49 and 0.78 Hz decreases with increasing distance from the plunging jet impact (Fig. 10B) and this is consistent with the wave amplitude decay associated with wave propagation, and observed during experiments Series 2.

Note that the writers do not explain the third energy peak around 1.5-2.5 Hz shown in Figure 10A.

5.2 Saltwater versus freshwater experiments

While present experiments were conducted with freshwater, seawater has different physical and chemical properties (e.g. RILEY and SKIRROW 1965). The difference in physical properties may affect the air entrainment, bubble breakup in the developing flow region, and the detrainment rate.

The quantity of entrained air may be estimated using Equation (2) and a change in inception velocity V_e associated with a change in fluid properties may affect the air entrainment rate. The difference between saltwater and freshwater density and surface tension is about +3% and +1% respectively at 20 Celsius and for 35 ppt salinity (e.g. CHANSON et al. 2002). This yields a negligible difference in inception velocity as predicted by CUMMINGS and CHANSON (1999) and observed by CHANSON et al. (2002).

In turbulent shear flows, a maximum air bubble size D_m may be estimated by the balance between the capillary force and the inertial force caused by the velocity change over distances of the order of the bubble diameter :

$$\frac{\rho_w * v^2 * D_m}{2 * \sigma} = (We)_c \quad (7)$$

CHANSON, H., AOKI, S., and MARUYAMA, M. (2002). "Unsteady Air Bubble Entrainment and Detrainment at a Plunging Breaker: Dominant Time Scales and Similarity of Water Level Variations." *Coastal Engineering*, Vol. 46, No. 2, pp. 139-157 (ISSN 0378-3839).

where σ is the surface tension between air and water, v'^2 is the spatial average value of the square of the velocity differences over a distance equal to D_m and $(We)_c$ is critical Weber number for bubble splitting (HINZE 1955). Experiments showed that the critical Weber number is a constant near unity (see reviews by EVANS et al. 1992, CHANSON 1995). Equation (7) implies that the maximum bubble size in salt water must be about 98% of the maximum size in freshwater shear flows.

For an individual air bubble rising uniformly in a fluid at rest and subjected to a hydrostatic pressure gradient, the rise velocity depends upon the value of the drag coefficient C_d which is a function of the bubble shape and velocity. Detailed reviews of rise velocity data include CLIFT et al. (1978) and COMOLET (1979). The results suggest little difference in bubble rise velocity between freshwater and saltwater. For small bubbles ($D_{ab} < 0.1$ mm), the rise velocity in salt water (20 Celsius, 35 ppt) is about 20% smaller than in freshwater, and the difference tends to zero for bubble sizes greater than 1 mm.

Overall the difference in physical properties between freshwater and saltwater might have little impact on the entrainment rate, bubble breakup and detrainment processes, but the topic requires a detailed, comparative study under controlled flow conditions.

6. Summary and conclusions

Physical modelling of a plunging breaker is traditionally conducted according to a Froude similitude. Scale effects may become significant in small size models because the breaker duration, bubble rise time and volume of entrained air cannot be properly scaled.

The unsteady air bubble entrainment at a pseudo-plunging breaking wave was physically modelled at near full-scale in laboratory. Experimental observations highlighted a number of unsteady air-water flow patterns : splashing at jet impact, underwater bubble plume, boiling region next to jet impact. The measurements emphasised high levels of aeration : i.e., depth-average void fraction of more than 10% next to jet impact in shallow waters. The results demonstrated that air entrainment in the surf zone is an important process by inducing a temporary water level rise and modifying the transmitted wave climate, and it cannot be ignored.

CHANSON, H., AOKI, S., and MARUYAMA, M. (2002). "Unsteady Air Bubble Entrainment and Detrainment at a Plunging Breaker: Dominant Time Scales and Similarity of Water Level Variations." *Coastal Engineering*, Vol. 46, No. 2, pp. 139-157 (ISSN 0378-3839).

Unsteady bubble injection was performed under controlled conditions. The experiments highlighted a very strong vortical motion induced by the rising bubbles. At the start of bubble injection, flow bulking and swarm circulation generated a positive wave propagating along the channel propagating at the celerity of a small disturbance ($\sqrt{g \cdot d_1}$). The water level rise (or superelevation) at the origin was associated with a water fall and local high velocities next to the free-surface for $X < 1$. At the end of bubble injection, a negative surge propagated in the channel with a rapid decay in circulation.

In summary the study contributes to a better understanding of unsteady bubble entrainment at a plunging jet and the associated vortical circulation, in part induced by the rising bubble swarm. But the pseudo-plunging jet had zero horizontal velocity component and model experiments started with the surrounding liquid initially at rest. In the field, plunging breakers are characterised by inclined plunging jets with time-varying jet impact conditions. Wave breaking near the coastline is also associated with significant sediment transport and the resulting flow becomes a three-phase flow: gas (air), liquid (water) and solid (sediment). The challenges ahead of fluid dynamics experts will be to comprehend the interactions between the three phases.

Acknowledgments

The authors acknowledge the financial support of the Australian Academy of Science, Japan Society for the Promotion of Science and Ministry of Education, Japan. They further thank the two reviewers, Dr J. GEMMICH and Dr H. OUMERACI, for their challenging and constructive comments.

Notation

B	channel width (m);
C	depth-averaged void fraction or air content;
d	water depth (m);
H	total head (m) above orifice;
L	length scale (m);

CHANSON, H., AOKI, S., and MARUYAMA, M. (2002). "Unsteady Air Bubble Entrainment and Detrainment at a Plunging Breaker: Dominant Time Scales and Similarity of Water Level Variations." *Coastal Engineering*, Vol. 46, No. 2, pp. 139-157 (ISSN 0378-3839).

L_T	geometric scaling ratio, defined as the ratio of prototype to model dimensions;
Q	water flow rate (m^3/s);
q_{air}	quantity of air entrained at the plunge point (m^2/s);
t	time (s);
T	dimensionless time : $T = t/(d_1/u_r)$;
T_{inj}	dimensionless bubble injection time;
T_{jet}	dimensionless duration of plunging breaker;
T_{22}	dimensionless time corresponding to the negative surge generated by end of bubble injection;
$T_{23\text{max}}$	dimensionless total duration of water level fluctuations associated with finite duration bubble injection;
t_{inj}	duration (s) of the air injection;
t_{jet}	duration (s) of the pseudo breaker;
u_r	bubble rise velocity (m/s) in still water;
V	plunging jet velocity (m/s) at nappe impact;
V_e	onset velocity (m/s) of air bubble entrainment at the plunge point;
w	vertical plume velocity (m/s);
x	horizontal distance (m);
X	dimensionless horizontal distance : $X = x/d_1$;
y	free-surface elevation (m) measured above the initial still water level;
Y	dimensionless free-surface elevation measured above still water level : $Y = y/d_1$;
$Y_{21\text{max}}$	dimensionless maximum water elevation following bubble injection;
$Y_{22\text{max}}$	dimensionless maximum amplitude of negative surge at end of bubble injection;

Symbols

\varnothing diameter;

CHANSON, H., AOKI, S., and MARUYAMA, M. (2002). "Unsteady Air Bubble Entrainment and Detrainment at a Plunging Breaker: Dominant Time Scales and Similarity of Water Level Variations." *Coastal Engineering*, Vol. 46, No. 2, pp. 139-157 (ISSN 0378-3839).

Subscript

R ratio of prototype-to-model quantity;

1 initial flow condition.

References

- AOKI, S., CHANSON, H., and MARUYAMA, M. (2000). "Water Level Rise Caused by Entrained Air Bubbles at Plunging Breakers: an Experimental Study" *Proc. 27th Intl Conf. Coastal Engineering*, Book of abstracts, Sydney, Australia, July 16-21, R. Cox Editor, Vol. 1, Poster 3, 2 pages.
- BIN, A.K. (1993). "Gas Entrainment by Plunging Liquid Jets." *Chem. Eng. Science*, Vol. 48, No. 21, pp. 3585-3630.
- CHANSON, H. (1995). "Hydraulic Design of Stepped Cascades, Channels, Weirs and Spillways." *Pergamon*, Oxford, UK, Jan., 292 pages.
- CHANSON, H. (1997). "Air Bubble Entrainment in Free-Surface Turbulent Shear Flows." *Academic Press*, London, UK, 401 pages.
- CHANSON, H. (1999). "The Hydraulics of Open Channel Flows : An Introduction." *Butterworth-Heinemann*, Oxford, UK, 512 pages.
- CHANSON, H., AOKI, S., and HOQUE, A. (2002). "Similitude of Air Bubble Entrainment and Dispersion in Vertical Circular Plunging Jet Flows. An Experimental Study with Freshwater, Salty Freshwater and Seawater." *Coastal/Ocean Engineering Report*, No. COE00-1, Dept. of Architecture and Civil Eng., Toyohashi University of Technology, Japan, 2002.
- CHANSON, H., and CUMMINGS, P.D. (1994). "Effects of Plunging Breakers on the Gas Contents in the Oceans." *Marine Technology Society Journal*, Vol. 28, No. 3, pp. 22-32.
- CHANSON, H., and LEE, J.F. (1997). "Plunging Jet Characteristics of Plunging Breakers." *Coastal Engineering*, Vol. 31, No. 1-4, July, pp. 125-141.

- CHANSON, H., AOKI, S., and MARUYAMA, M. (2002). "Unsteady Air Bubble Entrainment and Detrainment at a Plunging Breaker: Dominant Time Scales and Similarity of Water Level Variations." *Coastal Engineering*, Vol. 46, No. 2, pp. 139-157 (ISSN 0378-3839).
- CHANSON, H., AOKI, S., and MARUYAMA, M. (1999). "Air Bubble Entrainment at Plunging Breakers and its Effect on Long Period Waves: an Experimental study." *Coastal/Ocean Engineering Report*, No. COE99-1, Dept. of Architecture and Civil Eng., Toyohashi University of Technology, Japan, July, 41 pages.
- CLIFT, R., GRACE, J.R., and WEBER, M.E. (1978). "Bubbles, Drops, and Particles." Academic Press, San Diego, USA, 380 pages.
- COLES, K.A. (1967). "Heavy Weather Sailing." *Adlard Coles*, London, UK, 303 pages.
- COMOLET, R. (1979). "Sur le Mouvement d'une bulle de gaz dans un liquide." ('Gas Bubble Motion in a Liquid Medium.') *Jl La Houille Blanche*, No. 1, pp. 31-42 (in French).
- CUMMINGS, P.D., and CHANSON, H. (1999). "An Experimental Study of Individual Air Bubble Entrainment at a Planar Plunging Jet." *Chem. Eng. Research and Design*, Trans. IChemE, Part A, Vol. 77, No. A2, pp. 159-164.
- DANIIL, E.I., and GULLIVER J. (1991). "Influence of Waves on Air-Water Gas Transfer." *Jl of Envir. Engrg.*, ASCE, Vol. 117, No. 5, pp. 522-540.
- DEANE, G.B. (1997). "Sound Generation and Air Entrainment by Breaking Waves in the Surf Zone." *Jl Acoustical Society of America*, Vol. 102, No. 5, pp. 2671-2689.
- EVANS, G.M., JAMESON, G.J., and ATKINSON, B.W. (1992). "Prediction of the Bubble Size Generated by a Plunging Liquid Jet Bubble Column." *Chem. Eng. Sc.*, Vol. 47, No. 13/14, pp. 3265-3272.
- FUHRBOTER, A. (1970). "Air Entrainment and Energy Dissipation in Breakers." *Proc. Intl Conf. Coastal Eng.*, pp. 391-398.
- GRIFFIN, O.M. (1984). "The Breaking of Ocean Surface Waves." *Naval Research Lab. Memo.*, Report No. 5337, Washington, USA.
- HENDERSON, F.M. (1966). "Open Channel Flow." *MacMillan Company*, New York, USA.
- HINZE, J.O. (1955). "Fundamentals of the Hydrodynamic Mechanism of Splitting in Dispersion Processes." *Jl of AIChE*, Vol. 1, No. 3, pp. 289-295.
- HUGHES, S.A. (1993). "Physical Models and Laboratory Techniques in Coastal Engineering." *Advanced Series on Ocean Eng.*, Vol. 7, World Scientific Publ., Singapore.

- CHANSON, H., AOKI, S., and MARUYAMA, M. (2002). "Unsteady Air Bubble Entrainment and Detrainment at a Plunging Breaker: Dominant Time Scales and Similarity of Water Level Variations." *Coastal Engineering*, Vol. 46, No. 2, pp. 139-157 (ISSN 0378-3839).
- HWUNG, H.H., CHYAN, J.M., and CHUNG, Y.C. (1992). "Energy Dissipation and Air Bubbles Mixing inside Surf Zone." *Proc. 23rd Intl Conf. on Coastal Eng.*, ASCE, Venice, Italy, Vol. 1, Chap. 22, pp. 308-321.
- IPPEN, A.T. (1966). "Estuary and Coastal Hydrodynamics." *McGraw-Hill*, New York, USA.
- KANWISHER, J. (1963). "On the Exchange of Gases between the Atmosphere and the Sea." *Deep-Sea Research*, Vol. 10, pp. 195-207.
- KOLOVAYEV, P.A. (1976). "Investigation of the Concentration and Statistical Size Distribution of Wind-Producing Bubbles in the Near-Surface Ocean Layer." *Oceanology*, Vol. 15, pp. 659-661.
- KOMAR, P.D. (1998). "Beach Processes and Sedimentation." Prentice Hall, Upper Saddle River NJ, USA, 2nd edition, 544 pages.
- LIN, C., and HWUNG, H.H. (1992). "External and Internal Flow Fields of Plunging Breakers." *Experiments in Fluids*, Vol. 12, pp. 229-237.
- LONGUET-HIGGINS, M.S. (1988). "Mechanisms of Wave Breaking in Deep Water" in "See Surface Sound." *Kluwer Academic Publishers*, NATO ASI Series C, Vol. 238, B.R. Kerman editor, pp. 1-30.
- MARUYAMA, M. (2000). "Water Level Rise and its Propagation caused by Entrained Air Bubbles at Plunging Breakers." *Masters thesis*, Dept. of Architecture and Civil Engrg., Toyohashi University of Technology, Japan, 114 pages (in Japanese).
- MONTES, J.S. (1998). "Hydraulics of Open Channel Flow." *ASCE Press*, New-York, USA, 697 pages.
- NIELSEN, P. (1984). "Field Measurements of Time-Averaged Suspended Sediment Concentrations under Waves." *Coastal Engineering*, Vol. 8, pp. 51-72.
- PERLIN, M., HE, J., and BERNAL, L.P. (1996). "An Experimental Study of Deep Water Plunging Breakers." *Physics of Fluids*, Vol. 8, No. 9, pp. 2365-2374.
- RILEY, J.P., and SKIRROW, G. (1965). "Chemical Oceanography." *Academic Press*, London, UK, 3 volumes.
- SAWARAGI, T. (1995). "Coastal Engineering - Waves, Beaches, Wave-Structure Interactions." *Elsevier*, Developments in Geotechnical Engineering Series, No. 78, Amsterdam, The Netherlands, 479 pages.

CHANSON, H., AOKI, S., and MARUYAMA, M. (2002). "Unsteady Air Bubble Entrainment and Detrainment at a Plunging Breaker: Dominant Time Scales and Similarity of Water Level Variations." *Coastal Engineering*, Vol. 46, No. 2, pp. 139-157 (ISSN 0378-3839).

STRAUB, L.G., BOWERS, C.E., and TARAPORE, Z.S. (1959). "Experimental Studies of Pneumatic and Hydraulic Breakwaters." *Technical Paper No. 25*, Series B, St Anthony Falls Hyd. Lab., University of Minnesota, Minneapolis, USA, 49 pages.

THORPE, S.A. (1982). "On the Clouds of Bubbles formed by Breaking Wind Waves in Deep Water and their Role in Air-Sea Gas Transfer." *Phil. Trans. R. Soc. Lond.*, A304, pp. 155-210.

TULIN, M.P., and WASEDA, T. (1999). "Laboratory Observations of Wave Group Evolution, Including Breaking Effects." *Jl. Fluid Mech.*, Vol. 378, pp. 197-232.

WALLACE, D.W.R., and WIRICK, C.D. (1992). "Large Air-Sea Gas Fluxes associated with Breaking Waves." *Nature*, Vol. 356, 23 Apr., pp. 694-696.

WOOD, I.R. (1991). "Air Entrainment in Free-Surface Flows." *IAHR Hydraulic Structures Design Manual No. 4*, Hydraulic Design Considerations, Balkema Publ., Rotterdam, The Netherlands, 149 pages.

CHANSON, H., AOKI, S., and MARUYAMA, M. (2002). "Unsteady Air Bubble Entrainment and Detrainment at a Plunging Breaker: Dominant Time Scales and Similarity of Water Level Variations." *Coastal Engineering*, Vol. 46, No. 2, pp. 139-157 (ISSN 0378-3839).

Table 1 - Summary of experimental flow conditions

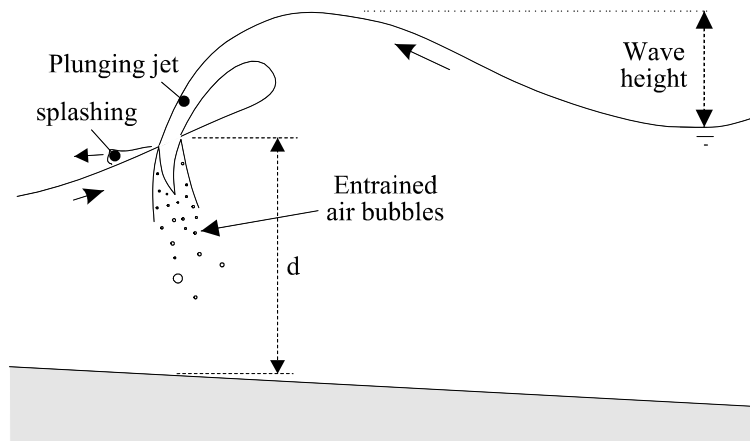
Exp.	Initial tank volume	Initial head above orifice H_1	Fall height orifice-bed	Initial flume conditions	Initial flow rate	Remarks
	m^3	m	m		$Q(t=0+)$ m^3/s	
(1)	(2)	(3)	(4)	(5)	(6)	(7)
Series 1						
1A	0.42 to 1.2	0.31 to 0.78	1.324	$d_1 = 0.2$ to 0.47 m $B = 0.8$ m	0.08 to 0.13	Free-falling jet. 33 experiments.
1B	0.42 to 1.2	0.31 to 0.77	1.324	$d_1 = 0.2$ to 0.47 m $B = 0.8$ m	0.10 to 0.16	Plastic cellophane sheets to suppress air entrainment. 20 experiments.
Series 2						
	N/A	N/A	N/A	$d_1 = 0.50$ m $B = 0.05$ m.	N/A	Bottom injection of air (37.3 l/min). 17 experiments.
2-1				No air injection		Sudden air injection ($t > 0$).
2-2				Continuous air injection		Sudden end of air injection ($t > 0$).
2-3				No air injection		Controlled air injection for $0 < t < t_{inj}$ with $1 \leq t_{inj} \leq 20$ s.

Notes : B : channel width; d_1 : initial flume water depth; H_1 : initial head in the reservoir; freshwater experiments.

CHANSON, H., AOKI, S., and MARUYAMA, M. (2002). "Unsteady Air Bubble Entrainment and Detrainment at a Plunging Breaker: Dominant Time Scales and Similarity of Water Level Variations." *Coastal Engineering*, Vol. 46, No. 2, pp. 139-157 (ISSN 0378-3839).

Fig. 1 - Plunging breaking waves

(A) Sketch of a plunging breaker



CHANSON, H., AOKI, S., and MARUYAMA, M. (2002). "Unsteady Air Bubble Entrainment and Detrainment at a Plunging Breaker: Dominant Time Scales and Similarity of Water Level Variations." *Coastal Engineering*, Vol. 46, No. 2, pp. 139-157 (ISSN 0378-3839).

(B) Wave breaking near the shoreline on the Gold Coast, Rainbow Beach after two days of big swell (Easter 2001) - End of a plunging breaker with surfers in front, Rainbow Beach, Gold Coast

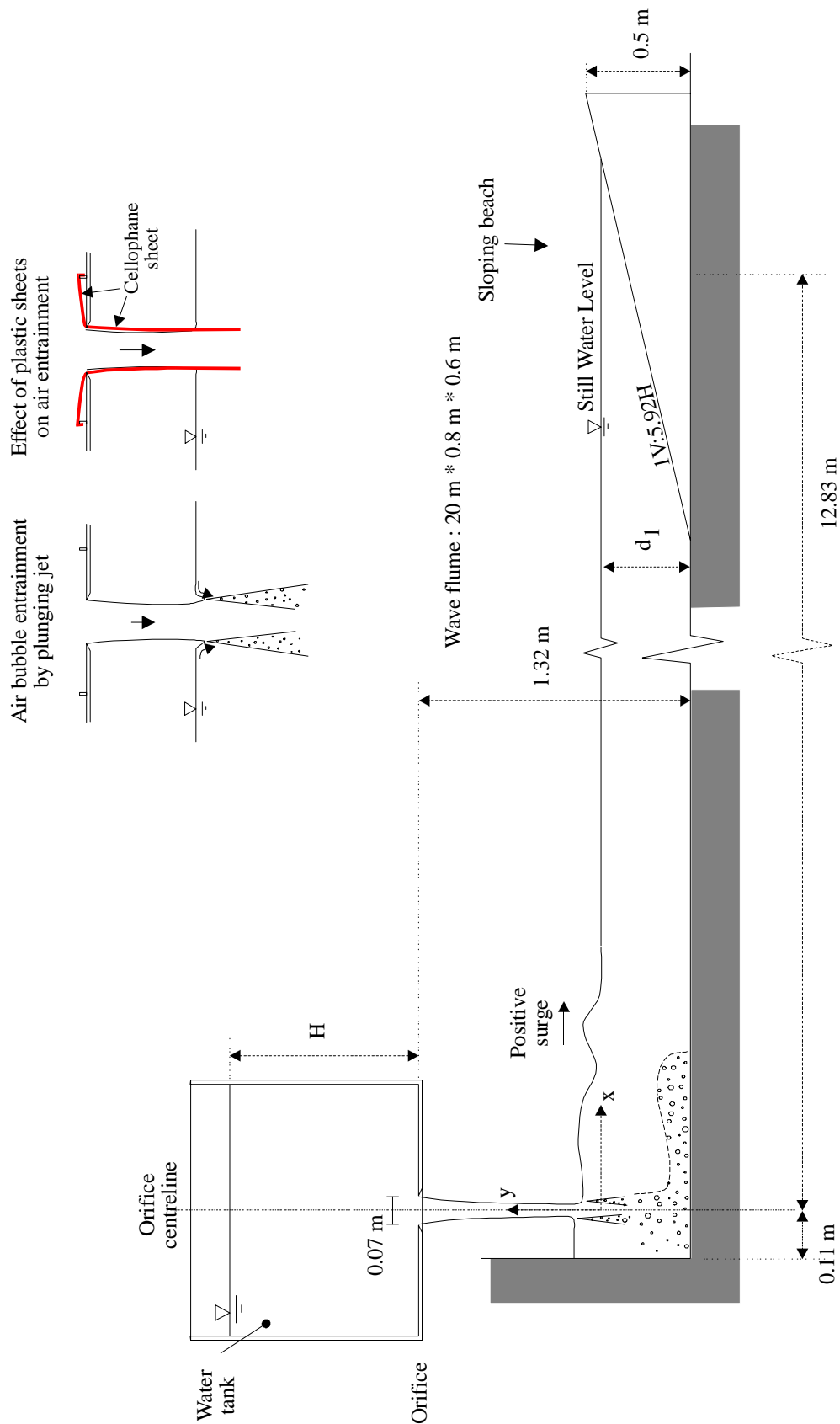


CHANSON, H., AOKI, S., and MARUYAMA, M. (2002). "Unsteady Air Bubble Entrainment and Detrainment at a Plunging Breaker: Dominant Time Scales and Similarity of Water Level Variations." *Coastal Engineering*, Vol. 46, No. 2, pp. 139-157 (ISSN 0378-3839).

Fig. 2 - Experimental facilities

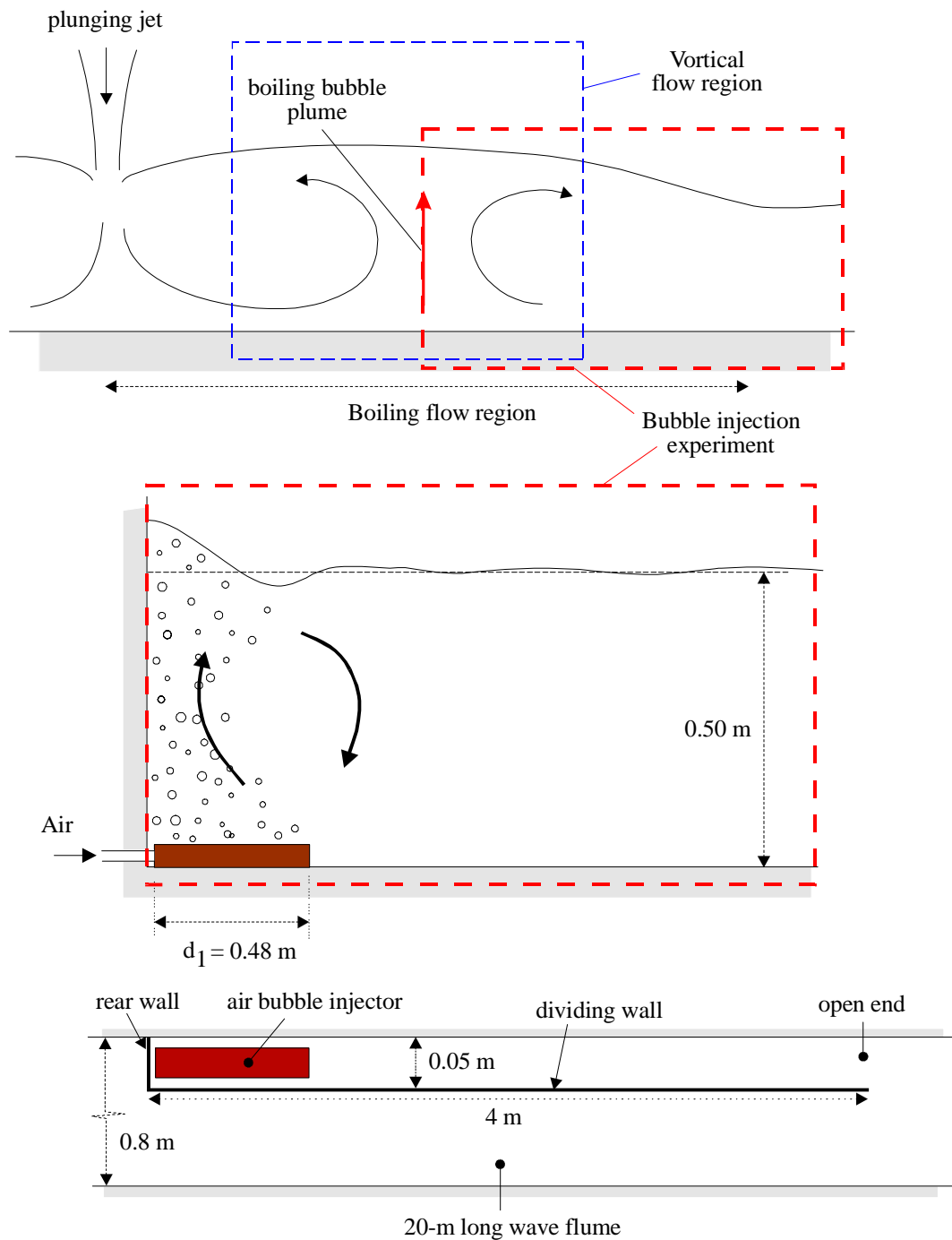
(A) First experimental facility

CHANSON, H., AOKI, S., and MARUYAMA, M. (2002). "Unsteady Air Bubble Entrainment and Detrainment at a Plunging Breaker: Dominant Time Scales and Similarity of Water Level Variations." *Coastal Engineering*, Vol. 46, No. 2, pp. 139-157 (ISSN 0378-3839).



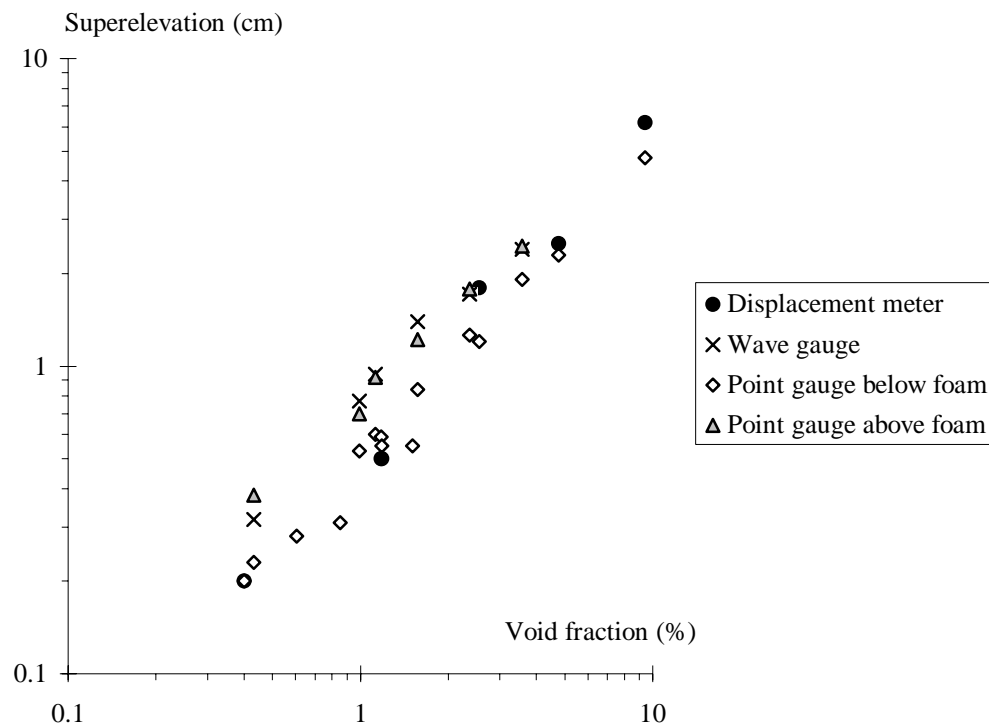
CHANSON, H., AOKI, S., and MARUYAMA, M. (2002). "Unsteady Air Bubble Entrainment and Detrainment at a Plunging Breaker: Dominant Time Scales and Similarity of Water Level Variations." *Coastal Engineering*, Vol. 46, No. 2, pp. 139-157 (ISSN 0378-3839).

(B) Second experimental facility



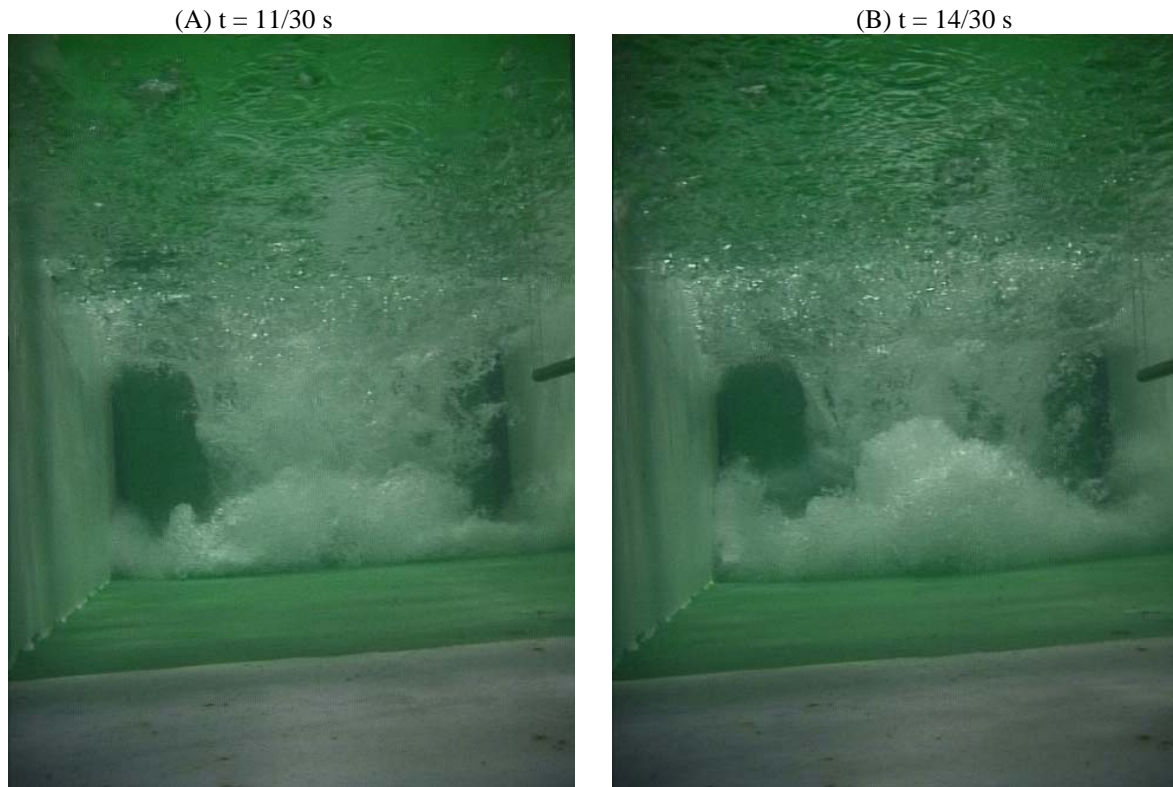
CHANSON, H., AOKI, S., and MARUYAMA, M. (2002). "Unsteady Air Bubble Entrainment and Detrainment at a Plunging Breaker: Dominant Time Scales and Similarity of Water Level Variations." *Coastal Engineering*, Vol. 46, No. 2, pp. 139-157 (ISSN 0378-3839).

Fig. 3 - Accuracy of capacitance water gauge and displacement meter in bubbly waters : superelevation (or water level rise above still water) as a function of the depth-averaged void fraction



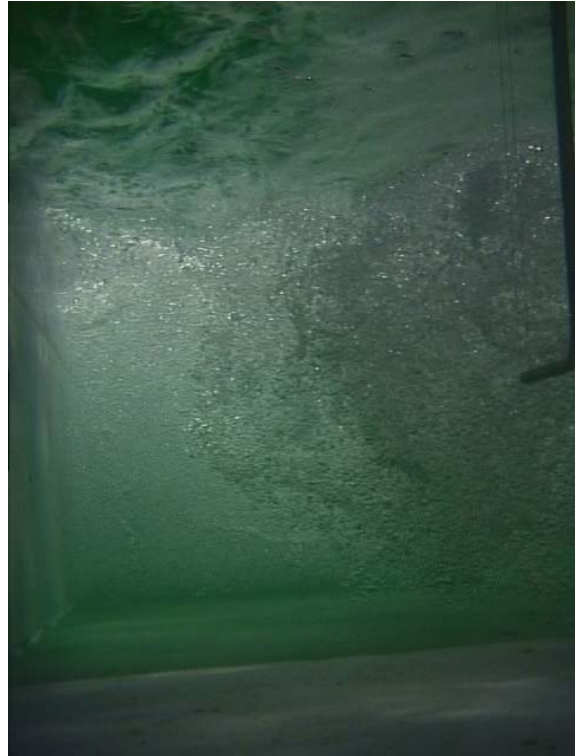
CHANSON, H., AOKI, S., and MARUYAMA, M. (2002). "Unsteady Air Bubble Entrainment and Detrainment at a Plunging Breaker: Dominant Time Scales and Similarity of Water Level Variations." *Coastal Engineering*, Vol. 46, No. 2, pp. 139-157 (ISSN 0378-3839).

Figure 4 - Underwater photographs of the bubbly plume - Initial water volume : 0.628 m^3 , $d_1 = 0.35 \text{ m}$ -
Camera located at $x \approx 2 \text{ m}$, looking toward the nappe impact



CHANSON, H., AOKI, S., and MARUYAMA, M. (2002). "Unsteady Air Bubble Entrainment and Detrainment at a Plunging Breaker: Dominant Time Scales and Similarity of Water Level Variations." *Coastal Engineering*, Vol. 46, No. 2, pp. 139-157 (ISSN 0378-3839).

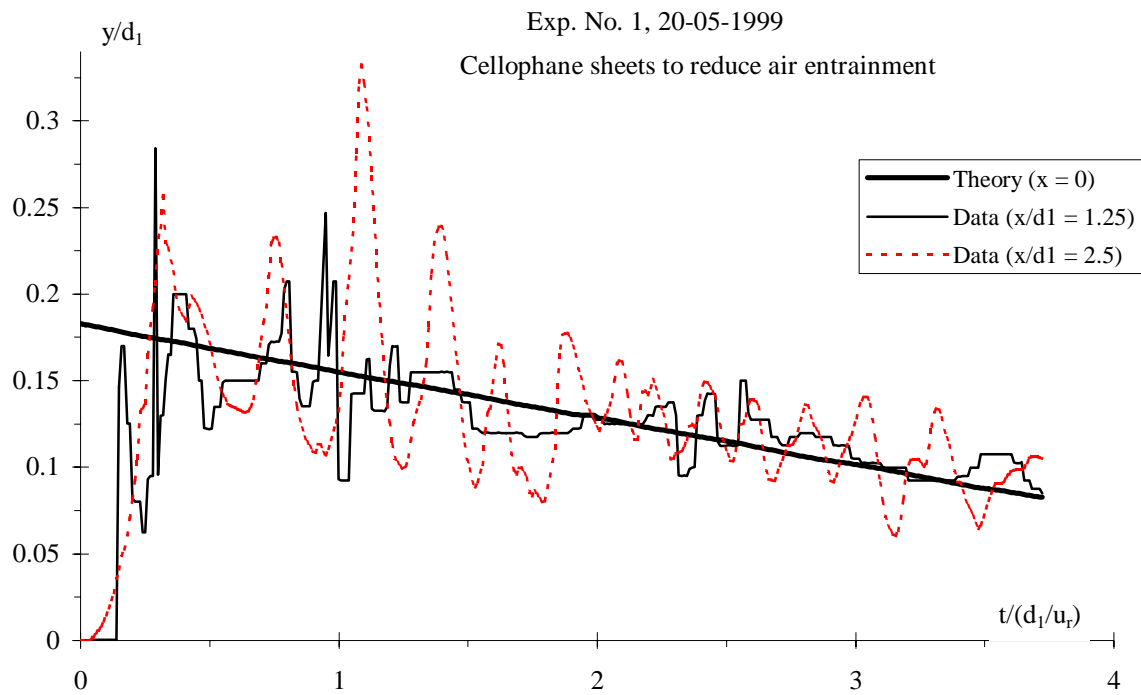
(C) $t = 16/30$ s (D) $t = 40/30$ s



CHANSON, H., AOKI, S., and MARUYAMA, M. (2002). "Unsteady Air Bubble Entrainment and Detrainment at a Plunging Breaker: Dominant Time Scales and Similarity of Water Level Variations." *Coastal Engineering*, Vol. 46, No. 2, pp. 139-157 (ISSN 0378-3839).

Fig. 5 - Comparison between observed water elevations and theoretical solution of the bore and negative surge at the origin

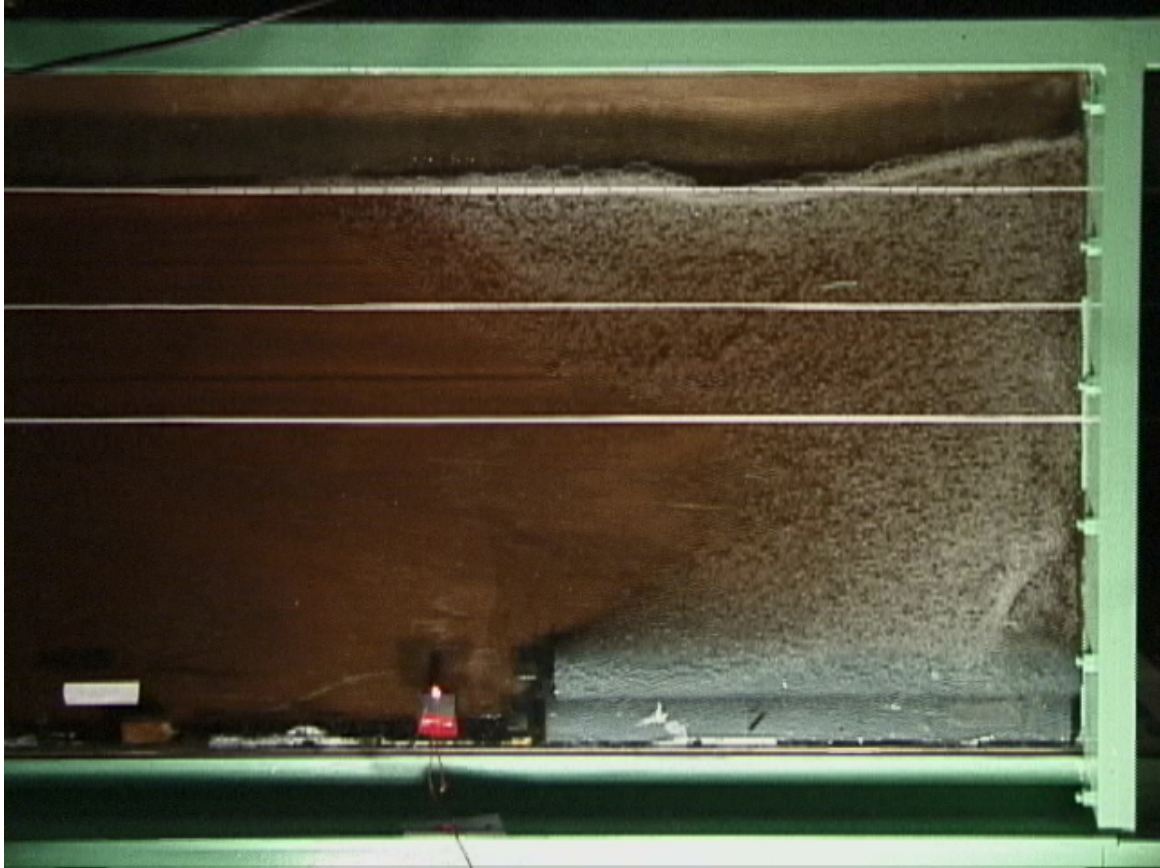
$H_1 = 0.571$ m, $d_1 = 0.40$ m, $u_r = 0.2$ m/s, Exp. No. 990520_1 with cellophane sheets to reduce air entrainment



CHANSON, H., AOKI, S., and MARUYAMA, M. (2002). "Unsteady Air Bubble Entrainment and Detrainment at a Plunging Breaker: Dominant Time Scales and Similarity of Water Level Variations." *Coastal Engineering*, Vol. 46, No. 2, pp. 139-157 (ISSN 0378-3839).

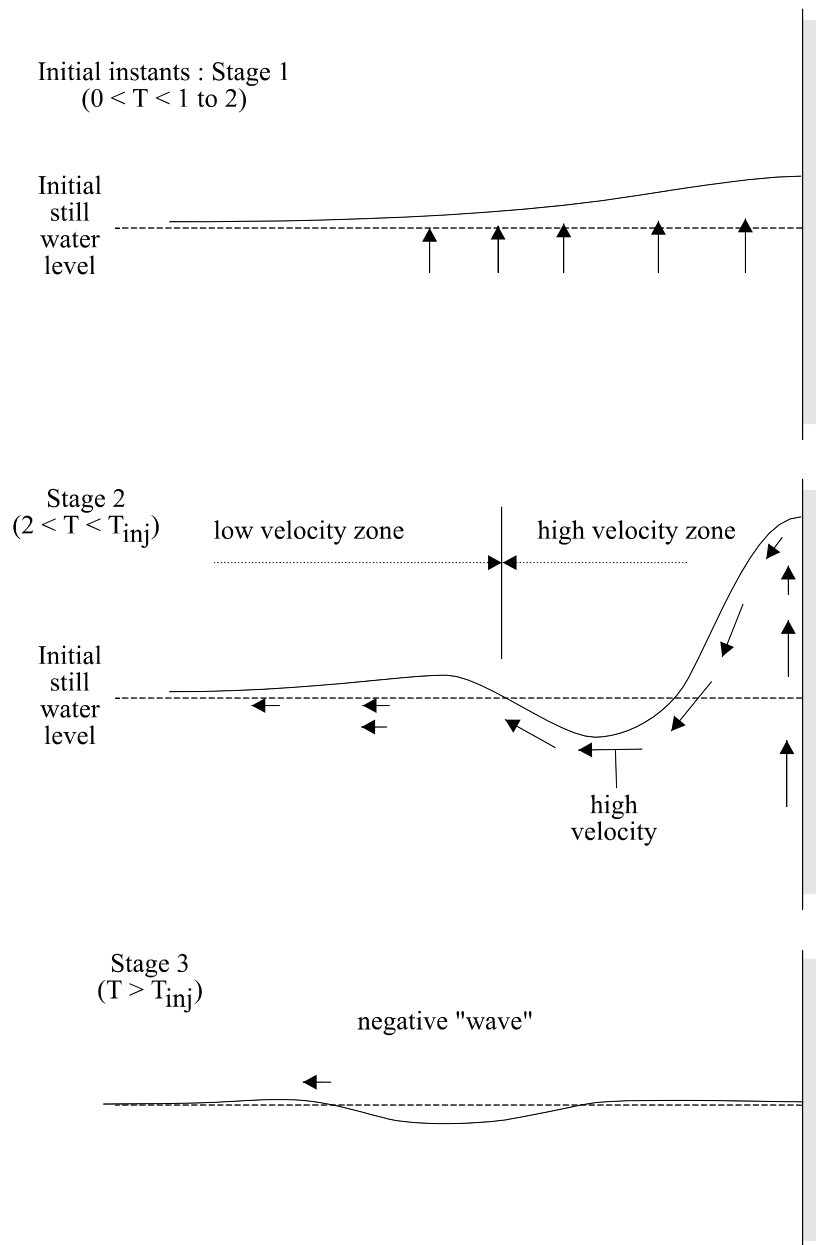
Fig. 6 - Free-surface levels in the air injection experiment (Series 2)

(A) Photograph taken at $t = 3$ s ($t_{inj} = 20$ s, $d_1 = 0.5$ m)



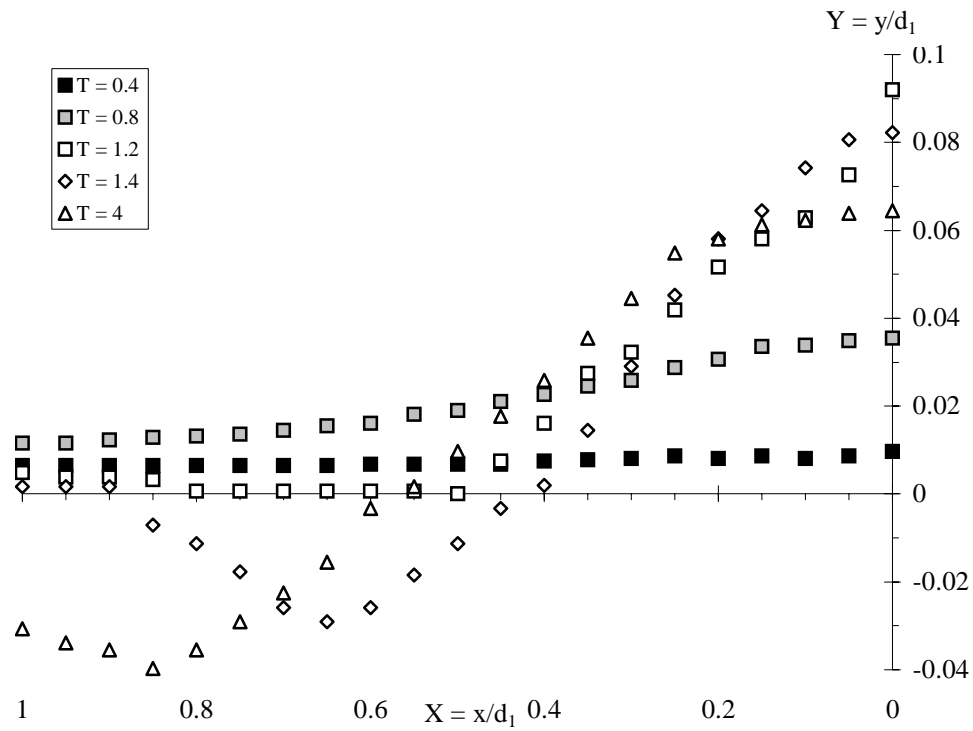
CHANSON, H., AOKI, S., and MARUYAMA, M. (2002). "Unsteady Air Bubble Entrainment and Detrainment at a Plunging Breaker: Dominant Time Scales and Similarity of Water Level Variations." *Coastal Engineering*, Vol. 46, No. 2, pp. 139-157 (ISSN 0378-3839).

(B) Sketch of free-surface flow pattern next to the injection point



CHANSON, H., AOKI, S., and MARUYAMA, M. (2002). "Unsteady Air Bubble Entrainment and Detrainment at a Plunging Breaker: Dominant Time Scales and Similarity of Water Level Variations." *Coastal Engineering*, Vol. 46, No. 2, pp. 139-157 (ISSN 0378-3839).

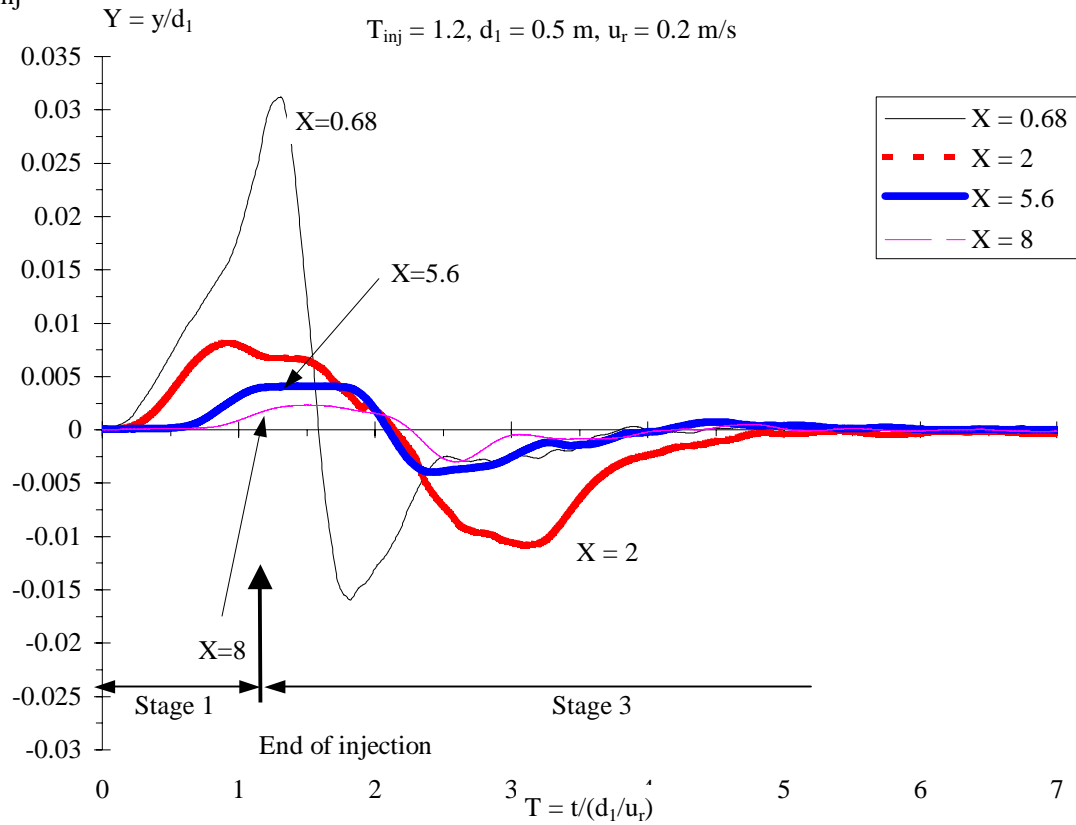
(C) Dimensionless free-surface elevations Y (measured above still water level) next to the origin after air bubble injection ($T_{inj} > 8$).



CHANSON, H., AOKI, S., and MARUYAMA, M. (2002). "Unsteady Air Bubble Entrainment and Detrainment at a Plunging Breaker: Dominant Time Scales and Similarity of Water Level Variations." *Coastal Engineering*, Vol. 46, No. 2, pp. 139-157 (ISSN 0378-3839).

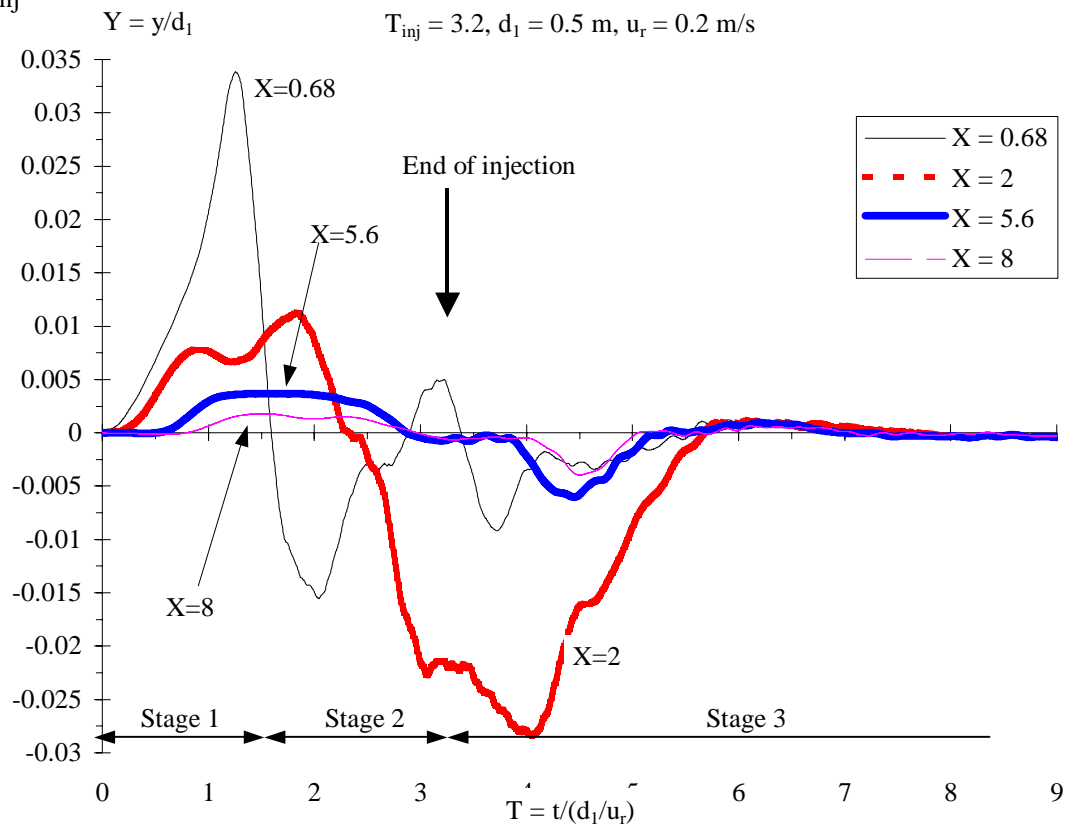
Fig. 7 - Time variations of dimensionless water levels (above still water) y/d_1 for different bubble injection times

(A) $T_{inj} = 1.2$



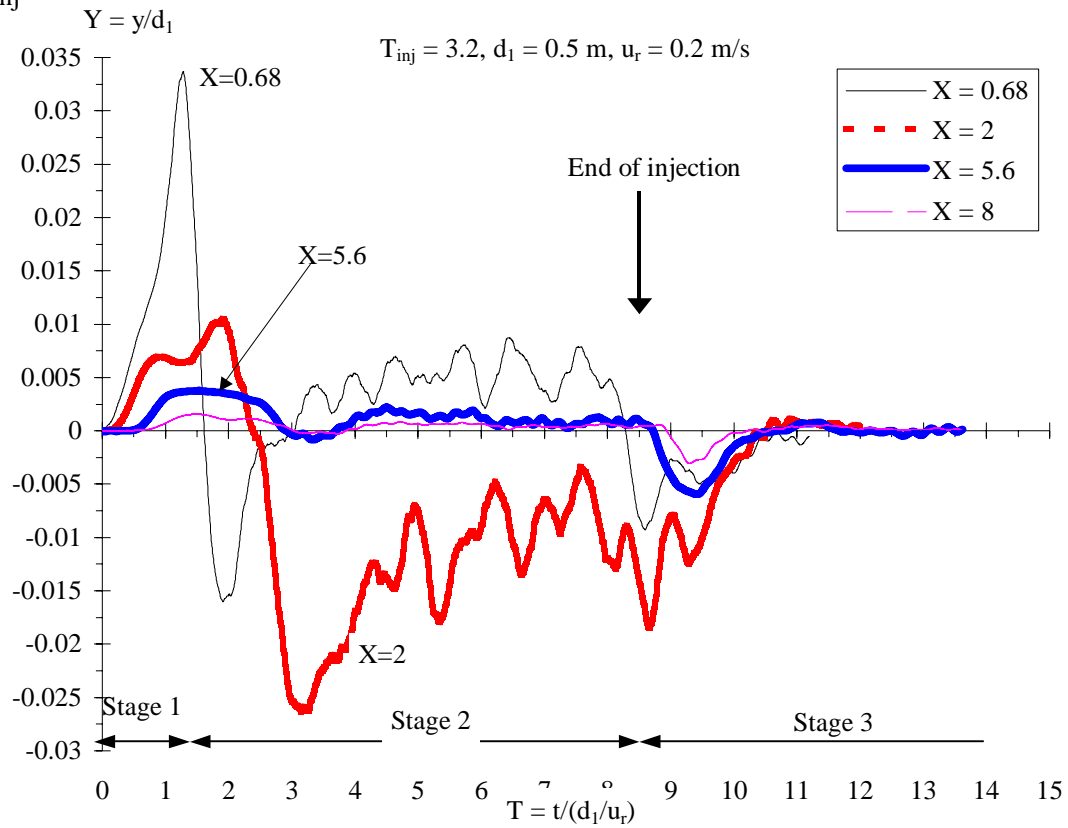
CHANSON, H., AOKI, S., and MARUYAMA, M. (2002). "Unsteady Air Bubble Entrainment and Detrainment at a Plunging Breaker: Dominant Time Scales and Similarity of Water Level Variations." *Coastal Engineering*, Vol. 46, No. 2, pp. 139-157 (ISSN 0378-3839).

(B) $T_{inj} = 3.2$



CHANSON, H., AOKI, S., and MARUYAMA, M. (2002). "Unsteady Air Bubble Entrainment and Detrainment at a Plunging Breaker: Dominant Time Scales and Similarity of Water Level Variations." *Coastal Engineering*, Vol. 46, No. 2, pp. 139-157 (ISSN 0378-3839).

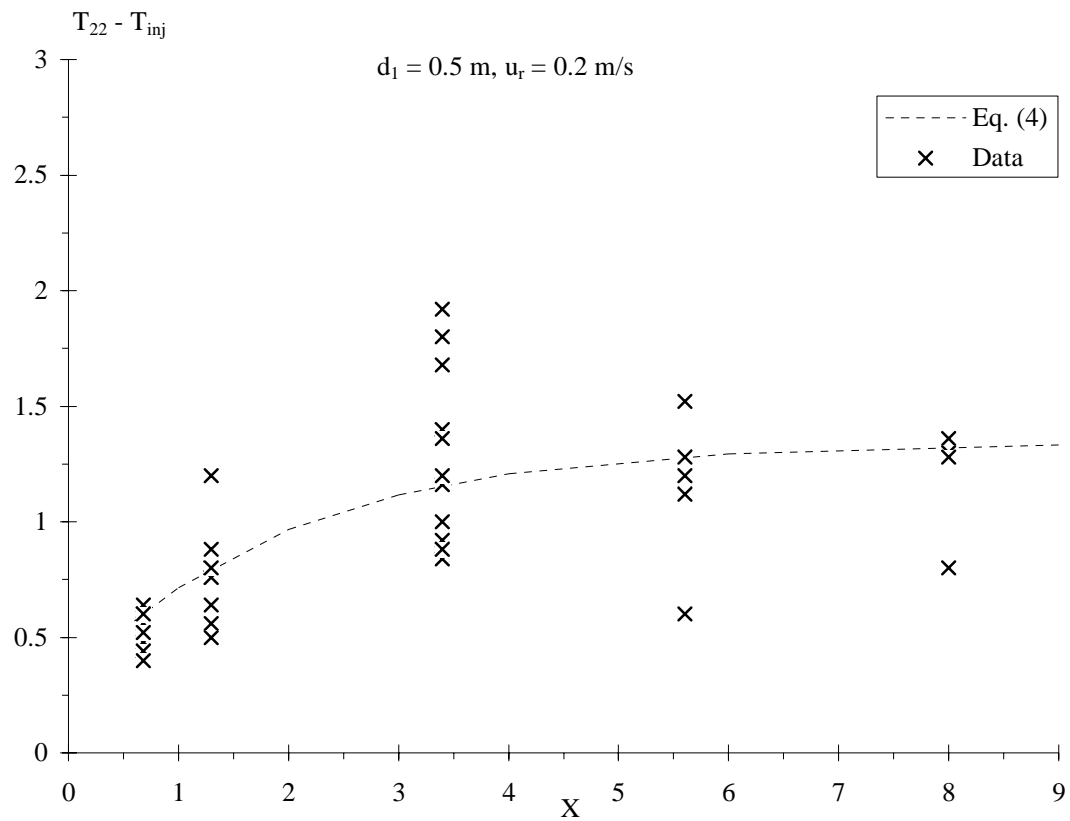
(C) $T_{inj} = 8.0$



CHANSON, H., AOKI, S., and MARUYAMA, M. (2002). "Unsteady Air Bubble Entrainment and Detrainment at a Plunging Breaker: Dominant Time Scales and Similarity of Water Level Variations." *Coastal Engineering*, Vol. 46, No. 2, pp. 139-157 (ISSN 0378-3839).

Fig. 8 - Dimensionless time T_{22} at which the maximum negative surge amplitude was observed

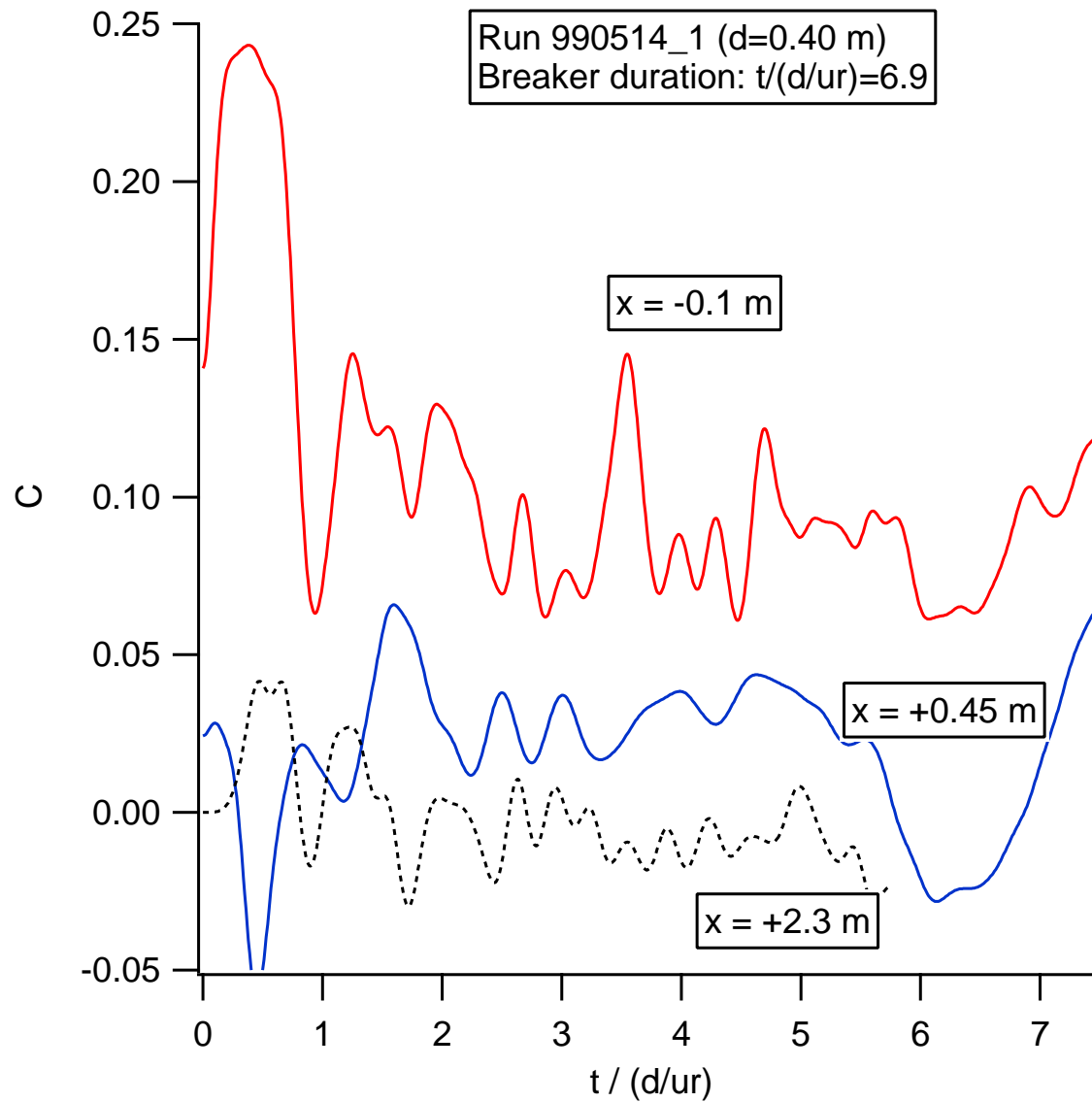
Comparison between experimental observations and Equation (4)



CHANSON, H., AOKI, S., and MARUYAMA, M. (2002). "Unsteady Air Bubble Entrainment and Detrainment at a Plunging Breaker: Dominant Time Scales and Similarity of Water Level Variations." *Coastal Engineering*, Vol. 46, No. 2, pp. 139-157 (ISSN 0378-3839).

Fig. 9 - Fluctuations of the depth-averaged void fraction at three longitudinal locations

$d_1 = 0.40$ m, Run 990514_1, breaker duration : $6.9 \cdot d_1 / u_r$, $u_r = 0.2$ m/s

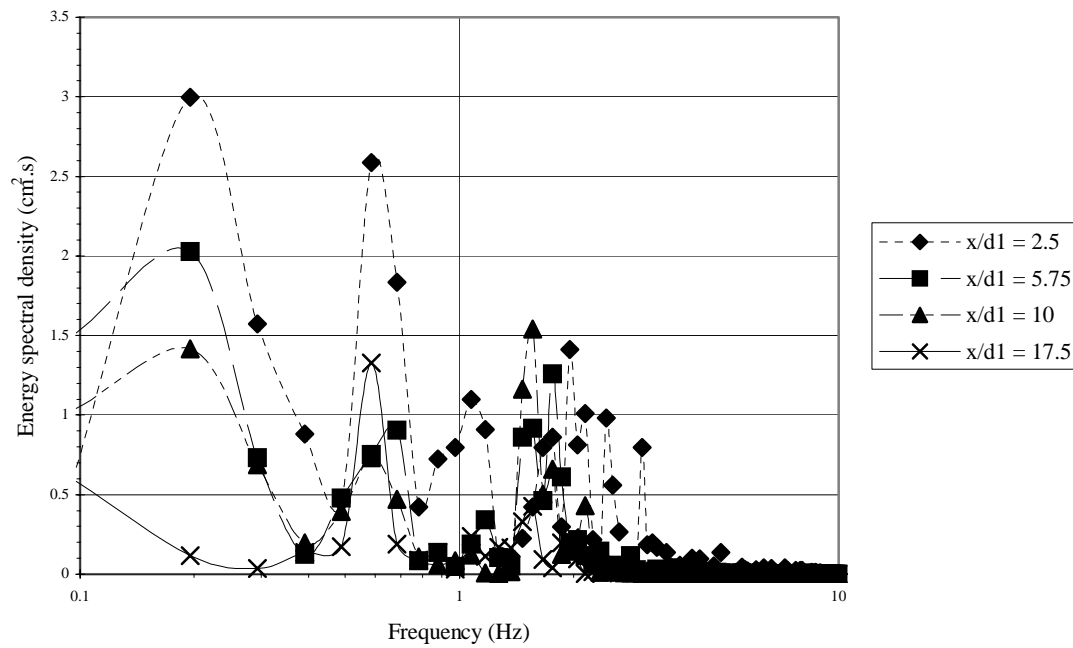


CHANSON, H., AOKI, S., and MARUYAMA, M. (2002). "Unsteady Air Bubble Entrainment and Detrainment at a Plunging Breaker: Dominant Time Scales and Similarity of Water Level Variations." *Coastal Engineering*, Vol. 46, No. 2, pp. 139-157 (ISSN 0378-3839).

Fig. 10 - FFT energy spectral density : {wave data with air entrainment} - {wave data with air entrainment suppression}

$H_1 = 0.57$ m, $d_1 = 0.40$ m - Wave gauges : $x = 1$ m, 2.3 m, 4 m, 7 m - {Exp. No. 990514_1} - {Exp. No. 990520-1}

(A) Energy spectral density



CHANSON, H., AOKI, S., and MARUYAMA, M. (2002). "Unsteady Air Bubble Entrainment and Detrainment at a Plunging Breaker: Dominant Time Scales and Similarity of Water Level Variations." *Coastal Engineering*, Vol. 46, No. 2, pp. 139-157 (ISSN 0378-3839).

(B) Ratio of Energy between 0.49 and 0.78 Hz to Total wave energy for experiment {990514_1} with air entrainment

